Optics Communications 369 (2016) 215–219

Contents lists available at ScienceDirect

Optics Communications

journal homepage: www.elsevier.com/locate/optcom

Effect of rotational wave packets on the stimulated emission of nitrogen with light filament

Ladan Arissian *, Brian Kamer, Amin Rasoulof

Center for High Technology Materials, 1313 Goddard SE, University of New Mexico, Albuquerque 87106, United States

ARTICLE INFO

Article history:
Received 14 October 2015
Received in revised form
22 February 2016
Accepted 23 February 2016
Available online 4 March 2016

Keywords:
Self-focusing, channeling, and filamentation in plasmas
Raman and Rayleigh spectra (including optical scattering)
Neutrals in plasmas

ABSTRACT

We measure forward emission of the nitrogen ion excited by light filaments at 800 nm. The radiation strongly depends on light polarization and orbital angular momentum. In all cases the rotational distribution of nitrogen molecules plays an essential role in the 428 nm stimulated emission.

1. Introduction

Light filaments [1], known as non-diffracting beams beyond multiple Rayleigh ranges, offer promising applications in remote sensing. The propagation of intense beam in air is affected by ionization, molecular and electronic Kerr effect, self phase modulation and diffraction [2,3]. Recently, there had been a great interest in controlling the stimulated emission in nitrogen molecular ions [4,5] and nitrogen neutral molecules [6–9]. We show the effect of rotational wave packet in enhancing the stimulated emission. The control of the rotational distribution of the medium is done in microscopic scale with light polarization (ellipticity) and in macroscopic scale using orbital angular momentum of light.

The phenomena contributing to the emission from filaments can be categorized as: (i) direct radiation from individual atoms or molecules (uni-molecular effects, including self-phase modulation, white light generation [10]), and (ii) amplification by a group of atoms/molecules, a collective phenomenon affected by light propagation. In the latter category one finds non-resonant effects (i.e. generation and amplification of new wavelengths by four wave mixing) and resonant effects (gain by population inversion). The amplification of a particular wavelength of the ultrashort pulse will proceed along a direction for which there is a group velocity matching [11] or Cherenkov radiation [12]. As in any laser without cavity, the process of amplification has to be seeded, either by vacuum fluctuation, spontaneous or conical emission.

The Kerr effect introduces spectral broadening through upchirp in gases with positive nonlinear index n_2, while the negative index plasma introduces a blue spectral shift [13]. Only a small percentage (0.01–0.1%) [14,15] of the molecules undergo ionization (higher electron densities are reported by Kandidov [16]). While air is an isotropic medium, its response is no longer isotropic when interacting with a polarized light. Strong field tunnel ionization results in a controlled electron trajectory that can be explored in the generation of THz radiation. Nitrogen and oxygen exhibit different polarizabilities along and perpendicular to their molecular axis. As the dipole interaction depends on the orientation of a molecule with respect to the field, there is a preferential ionization [17] along the light polarization. For neutral molecules in air and also for ions, there is a torque proportional to the projection of the dipole moment along the light polarization $pE\cos\theta$, in which p is the polarizability, E the electric field and θ the angle between the two vectors. In a non-perturbative approach the laser field is treated classically and material quantum mechanically. The rotational distribution (in "J's") is modified from its Boltzman distribution due to the light interaction, and for light the medium is birefringent. For pulses shorter than the rotational period of the molecule (8.4 ps for nitrogen), a rotational wavepacket is generated, resulting in field-free alignment at delays corresponding to multiple integers of the rotational period [18,19]. Transient birefringence is observed over the length of a single ultrashort pulse, leading to polarization modification of the pulse itself [20].

A simple setup is chosen for the investigation of forward radiation caused by light filaments, as shown in Fig. 1. The 428 nm radiation is collected by a monochromator with a CCD camera

* Corresponding author.
E-mail address: ladan@unm.edu (L. Arissian).

http://dx.doi.org/10.1016/j.optcom.2016.02.052
0030-4018/

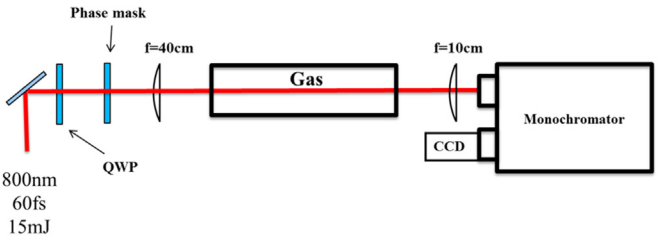

Fig. 1. Setup to study the forward emission at 428 nm generated in a N_2 filled cell (1 atm pressure) by a filament created with 15 mJ, 60 fs pulses at 800 nm (10 Hz repetition rate). The light polarization is controlled by a quarter wave plate and its orbital angular momentum can be changed with a spiral phase plate. The light is focused (NA=0.19) into the cell. The transmitted light is focused by a $f=10$ cm fused silica lens onto the entrance slit of a spectrometer, calibrated with a mercury lamp using the spectral lines at 404.66 and 435.84 nm.

placed at its exit. The image on the CCD spans a 42 nm bandwidth and is centered at 426 nm with the pixel resolution of 0.0088 nm. The spectrometer is a coma-aberration corrected Czerny–Turner configuration with focal length of 0.64 m. The image is taken with a Thorlabs CCD of 4872 × 3248 pixels (16 000m-00-GE). For each measurement the image is integrated for 10 s to have a comparable image under various conditions. The two dimensional image on the CCD is integrated along the vertical axis and presented as a signal versus wavelength.

The forward emission at 428 nm is shown in Fig. 2(a) and (b). Similar results had been recently published [21]. The inset in Fig. 2 (a) indicates the spectroscopic ro-vibrational branches of transitions between the $B^2\Sigma_u^+\nu' = 0$ to $X^2\Sigma_g\nu'' = 1$, where ν is the vibrational quantum number. The integrated signal is presented as function of wavenumber (cm^{-1}), in which zero corresponds to 23 374 cm^{-1} (P transition to $J=5$). Throughout the paper the rotational lines are defined with the final state of J, so the P transition $J' = 4 \rightarrow J'' = 5$ is labeled $J=5$. At first glance the spectrum of Fig. 2(a) may be mistaken as a rotational Raman spectrum with $\Delta J = 2$. Our measurements show the direct transition of the R branch to be an order of magnitude stronger than the Raman transition of the S branch. Direct emission transitions sketched in Fig. 2(a) comprise a P branch ($\Delta J = -1$), and an R branch ($\Delta J = +1$). The generated 428 nm light undergoes Raman transition during propagation, with the emission of an O-branch ($\Delta J = 2$) and an S-branch ($\Delta J = -2$). The energy levels (in cm^{-1}) are given by:

$$E = \omega_e\left(\nu + \frac{1}{2}\right) - \chi_e\omega_e\left(\nu + \frac{1}{2}\right)^2 + Y_e\omega_e\left(\nu + \frac{1}{2}\right)^3 + B_\nu J(J+1) - D_e J^2(J+1)^2 + T_e. \quad (1)$$

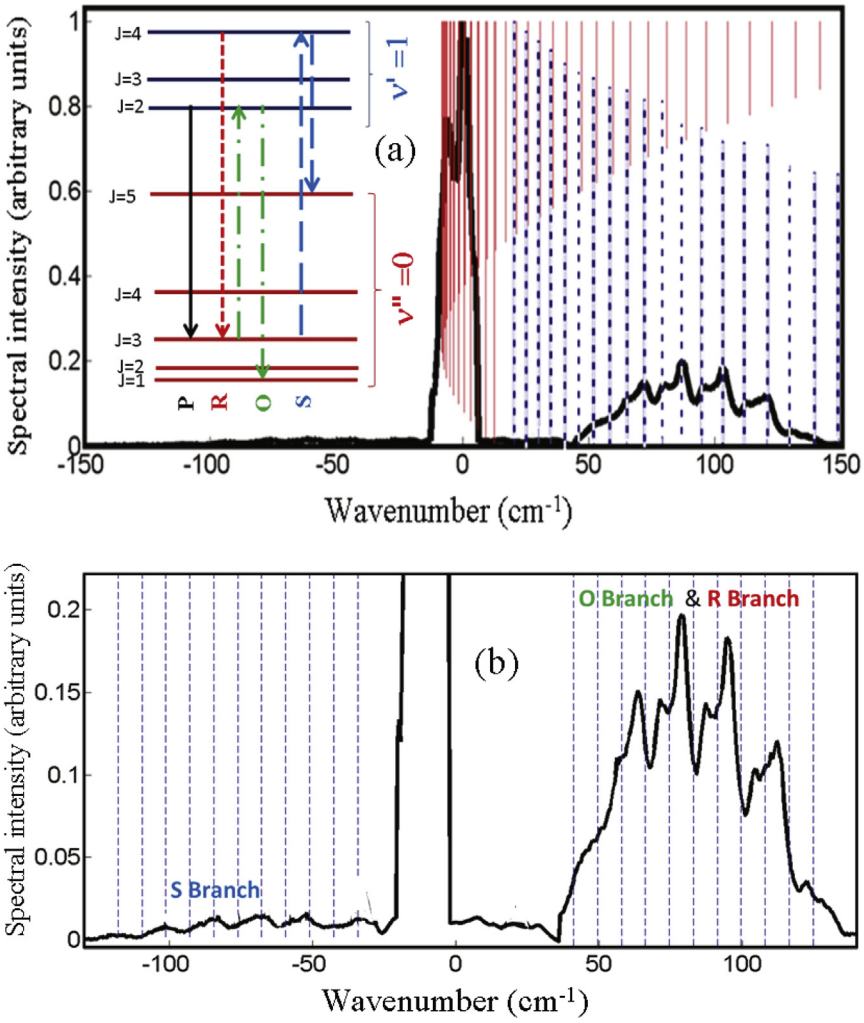

Fig. 2. Time integrated spectral intensity around 428 nm, compared to the calculated lines based on Eq. (1). The P branch starts from $J=0$; the R branch from $J=1$. (a) The resolved lines are in agreement with P and R lines shown in red (solid lines) and blue (dashed) respectively. Multiple rotational lines can fit under the P branch. The inset shows the spectroscopic vibrational transitions (from upper state ν' to lower state ν'') of photons between various rotational states. (b) The same image is zoomed in and compared with Raman lines of X state with $\Delta J = 2$ [O branch (right)] and $\Delta J = -2$ [S branch (left)]. (For interpretation of the references to color in this figure caption, the reader is referred to the web version of this paper.)